(Received 27 December 2023, Accepted 23 January 2024, Scheduled 15 February 2024)

Advancing Wireless Connectivity: A Dual-Band Microstrip Antenna Enhanced by Hexagon Cell Reflector for Superior Gain and Directivity

Maniram Ahirwar* and Virendra S. Chaudhary

Department of Electronics and Communication Engineering, RKDF University, Gandhinagar, Bhopal, India

ABSTRACT: In this exploration, our focus lies on unveiling a novel Mixed Multi-Elliptical Shaped (MMES) microstrip patch antenna, notably compact in design. Using the co-planar waveguide (CPW) port technique on an FR-4 substrate, we introduce an antenna showcasing a dual fractional bandwidth. Remarkably, and it spans 76.95% from 2.87 to 6.5 GHz and 53.85% from 8.06 to 14 GHz. To enhance both Gain and Directivity, our design integrates a Hexagon Cell with an Octagon Slot array reflector. This addition results in a peak gain of 8.759 dBi and a maximum directivity of 9.537 dBi at 6 GHz. Achieving optimal Gain and Directivity involved precise adjustments to the gap between the antenna and reflector plane. The overall dimensions of our proposed antenna measure $59 \times 59 \times 11.67\,\text{mm}^3$. Rigorous simulations and empirical validation strongly support the potential of this antenna for applications in BT, WLAN, and WiMAX.

1. INTRODUCTION

Monopole microstrip antennas provide value since they are compact, low profile, and easy to build. They may also be easily included on a circuit board. Numerous wireless applications face hindrances in deployment, stemming from constraints like restricted bandwidth, subpar gain, and diminished directivity. Despite decades of extensive development, microstrip patch antennas have achieved only modest gains. Even with conventional substrate materials, the maximum attainable gain typically hovers in the range of 5–8 dBi. Many applications benefit from planar radiating apertures with high gains and low side lobe level (SLL) [1–5]. Millimetre wave wireless systems, for example, have recently attracted a lot of attention as a result of the ever-increasing need for high data rates. Because of the large propagation loss in short-range wireless communications such as Wi-Fi, printed antennas with high gain are necessary; hence, the 60 GHz millimetre wave unlicensed band is an ideal option. Various methods exist for enhancing the gain of microstrip patch antennas. These include: 1) Utilizing substrates with low dielectric constants like foam or honeycomb, 2) employing array designs, 3) integrating metasurfaces, 4) incorporating fractal boundary antennas, and 5) applying reflective surface patterns. Nevertheless, foam and honeycomb bases have fallen out of favor due to their intricacy and elevated expenses. Recently, there has been a surge in interest in employing Partially Reflective Surfaces as outer layers in constructing high-gain planar antennas [6–9]. These antennas are alternately referred to as Fabry-Perot cavity antennas or cavity resonance antennas. They offer an edge over microstrip arrays as they do not necessitate an intricate feed network. Using this setup, a lot of money has been made [10, 11]. Good gain, which increases the total antenna profile, can only be obtained by positioning the PRS superstrate about 0.5λ above the ground plane. Several studies have been conducted to investigate strategies to minimize profile utilizing AMCs and metamaterials on top of AMCs [12–15].

* Corresponding author: Maniram Ahirwar (maniram.ahirwar@mp.gov.in).

2. DESIGNING THE ANTENNA

The presented design of the patch antenna and reflector will affect its properties, such as its resonant frequency, bandwidth, gain, and radiation pattern. The dimensions of the patch, the thickness and dielectric constant of the substrate, the type of feed used, and the size and shape of the reflector will all influence these properties.

Here are some of the key features of the patch antenna with reflector shown in the figures:

Rectangular Patch: This is the most common type of patch antenna. The length and width of the patch are determined by the desired resonant frequency of the antenna.

Feed: Feed is the point at which the antenna is connected to the transmission line. There are many different types of feeds, but the most common are coaxial feeds and microstrip feeds.

Substrate: Substrate is typically made of a material with a low dielectric constant, such as FR4. The thickness of the substrate also affects the resonant frequency of the antenna.

Reflector: Reflector is a conducting surface that is placed behind the patch. It is usually made of copper and is shaped to reflect the microwaves emitted by the patch in a particular direction. This can be used to increase the gain of the antenna in a particular direction or to reduce the amount of radiation in other directions [16, 17].

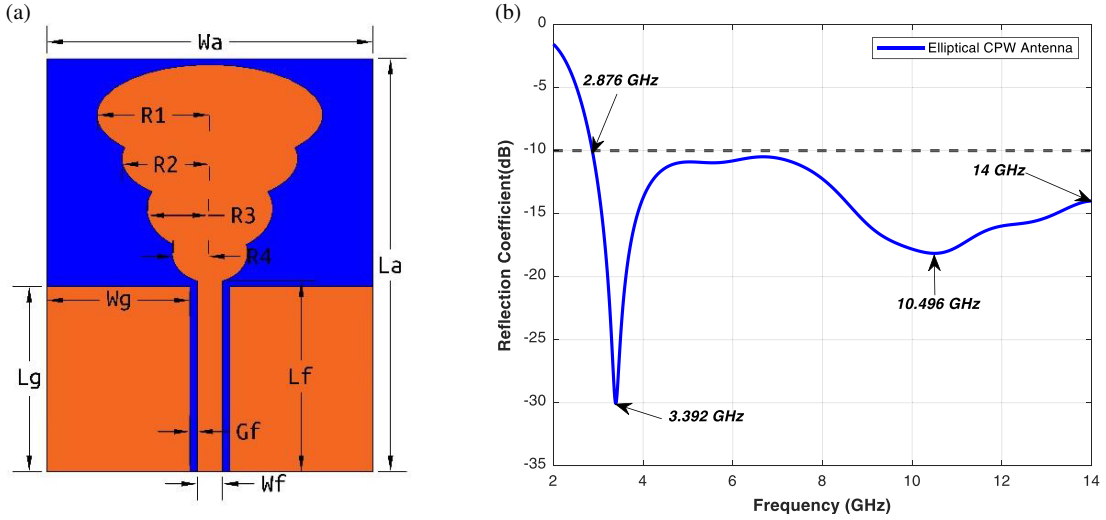

FIGURE 1. (a) Structure of mixed multi-elliptical shaped microstrip CPW antenna. (b) Reflection coefficient characteristics (S_{11}) of mixed multi-elliptical shaped microstrip CPW antenna.

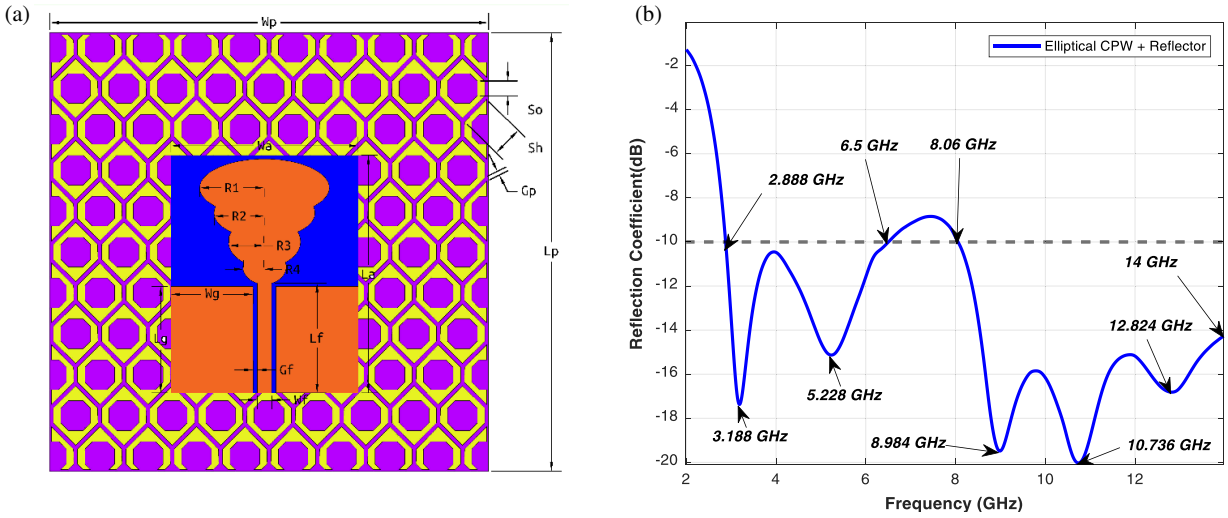

FIGURE 2. (a) Illustrating the configuration of a microstrip antenna with an elliptical shape, augmented by a hexagonal cell and an octagonal slot reflector. (b) Analyzing the Reflection Coefficient characteristics (S_{11}) of a hybrid multi-elliptical-shaped microstrip antenna on a CPW substrate, enhanced with a specialized reflector.

This innovative design incorporates a mixed, multi-elliptical-shaped microstrip antenna, enhanced by a hexagon cell with an octagon slot reflector array. The meticulously engineered antenna configuration is illustrated in Figure 1. This ensemble is meticulously crafted on an FR-4 substrate with a thickness of 1.6 mm, boasting a minimal loss tangent $(\tan(\delta))$ of 0.02 and a dielectric constant (ε_r) of 4.3. In the design of the antenna, a sophisticated radiating element with a Mixed Multi-Elliptical Shape is intricately woven into the structure, strategically linked to a 50 Ω microstrip feed line. This deliberate connection guarantees an exact impedance match between the patch and the source. Moreover, the coplanar rectangular shape of the ground element structure has been seamlessly integrated on both sides of the feed, enhancing its overall functionality. The designed antenna consists of both the patch and ground planes in the same plane, and a coplanar waveguide feed (CPW) port is used to provide the source. Fine-tuning the dimensions of the radiating patch, the width of the feed line, and the ground elements has resulted in achieving the ideal impedance matching crucial for excellent reflection coefficient characteristics in the presented antenna design. This optimized setup ensures effective coupling between the radiating patch and the ground. The physical parameters of the antenna measure $26 \times 33 \times 1.6\,\text{mm}^3$, as detailed in Table 1. Enhancing both the Gain and Directivity, a hexagonal cell with an array reflector comprising octagon slots has been integrated into the antenna design. The overall dimensions of the proposed antenna structure measure $59 \times 59 \times 11.67\,\text{mm}^3$, as illustrated in Figure 2. For a more detailed breakdown of the antenna's dimensions, please refer to Table 1.

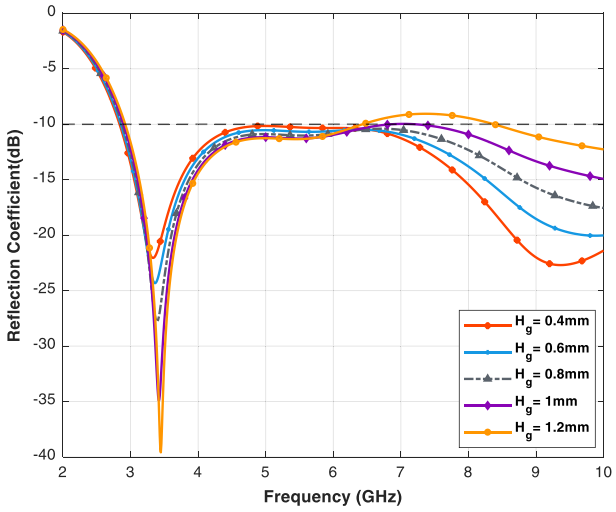

FIGURE 3. Impact of height of ground (H_g) on return loss characteristics (S_{11}).

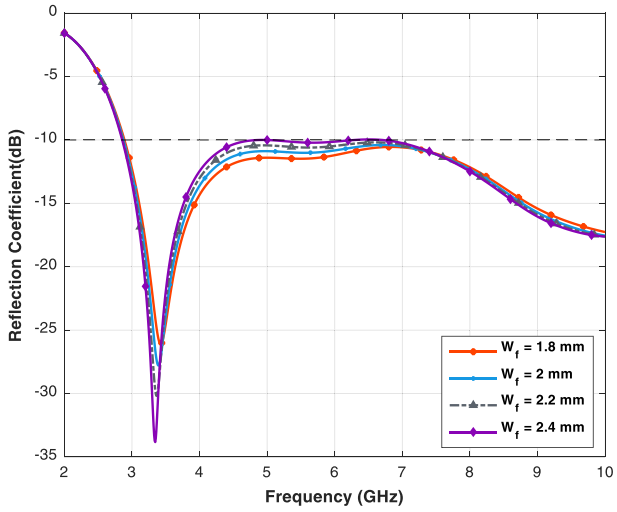

FIGURE 4. Impact of microstrip feed line width (W_f) on return loss characteristics (S_{11}).

TABLE 1. Dimension details of the proposed antenna.

Dimension	Value(mm)	Dimension	Value(mm)
Wa	26	*Wp*	59
La	33	*Lp*	59
R1	8.93	*So*	2
R2	6.95	*Sh*	4.21
R3	4.82	*Gp*	0.56
R4	2.83	*Gap*	10
Lf	15.24	*Lg*	14.8
Wf	2	*Gf*	0.6
Wg	11.4		

The lower cut-off frequency is $f_{\text{low}} = 4.125$ GHz, and the higher cut-off frequency is $f_{\text{high}} = 10$ GHz. The first resonance frequency $f_{r1} = 5.092$ GHz and $f_{r2} = 9.172$ GHz with a maximum return loss of -15.0299 dB and -28.159 dB, respectively.

3. PARAMETRIC ANALYSIS

Parametric analysis is the most important kind of analysis for reaching the presented antenna to its optimum level in terms of the physical structure of the designed antenna. In this section, antenna parameters have been tuned within a specific range. The changes are made one at a time to see how they affect antenna performance in terms of correct impedance matching and achieving good reflection coefficient $|S_{11}|$ characteristics. The parametric analysis has been done with the parametric sweep function provided by CST studio.

3.1. Effect of Ground Height ($H_g = 14.4$ to 15.20 mm)

Variations in ground height (H_g) play a pivotal role, fluctuating between 14.4 mm and 15.20 mm, significantly impacting the ideal impedance matching between the radiating patch and the ground plane. This measurement signifies the distance separating the underside of the radiating patch from the upper surface of the ground. Specifically, when H_g equals 14.80 mm, a space of 0.5 mm emerges between the radiating patch and the ground, optimizing the curve of the reflection coefficient. Figure 3 visually captures the impact of ground height (H_g) on the antenna's overall performance.

3.2. Microstrip Feed Line Width: Implications and Influence ($W_f = 1.8$ to 2.4 mm)

The width (W_f) of the microstrip feed line plays a pivotal role by establishing crucial impedance matching between the radiating patch and its source. This parameter holds immense significance in ensuring optimal performance within the system. For this study, a 50 Ω microstrip feed line was selected, and its dimensions were adjusted within the range of 1.8 mm to 2.4 mm. The variation has been performed and found that a very small change has been recorded in lower cutoff (f_{low}) and higher cutoff (f_{high}) frequencies and observed that the high dip in reflection characteristics below -25 dB had been found at the value 1.8 mm at 3.4 GHz. Figure 4 exhibits how the antenna performance is influenced by variations in feed width.

3.3. Microstrip Feed Line Length: Implications and Influence ($L_f = 13.24$ to 17.24 mm)

The dimension known as the width of the microstrip feed line (L_f) plays a crucial role by enabling the proper matching of impedance between the radiating patch and the energy source. A 50 Ω microstrip feed line was adopted, and its dimensions were adjusted within the range of 13.24 mm to 17.24 mm. The variation has been performed and found that a change has been recorded in lower cutoff (f_{low}) frequency and also observed that the high reflection characteristics were obtained at the value of 15.24 mm. Figure 5 shows the impact of feed length on antenna performance.

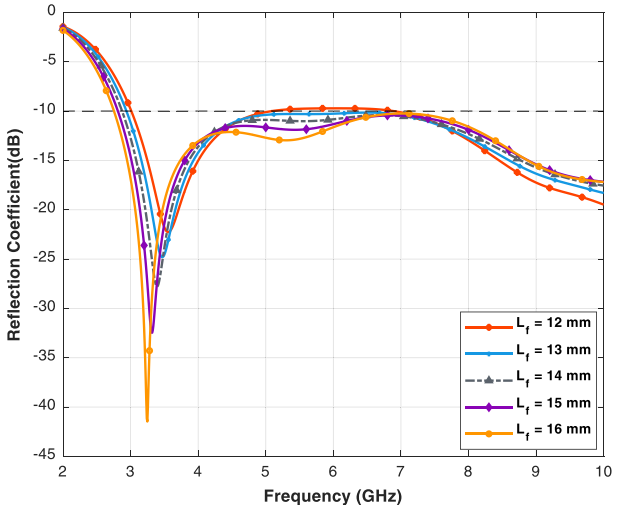

FIGURE 5. Impact of microstrip feed line length (L_f) on return loss characteristics (S_{11}).

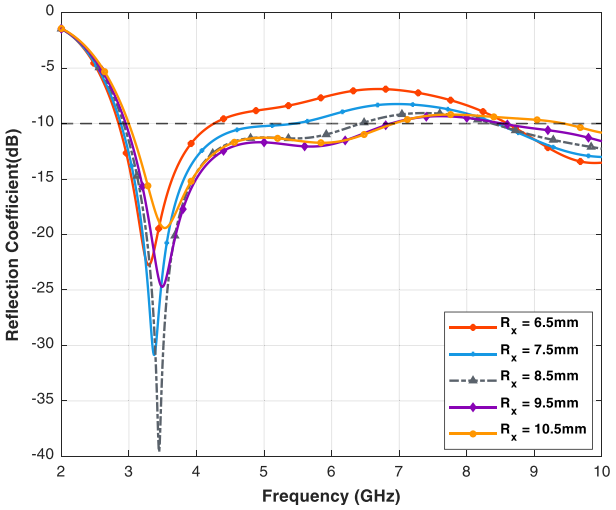

FIGURE 6. Impact of circular patch element radius (R_X) on return loss characteristics (S_{11}).

(a)

(b)

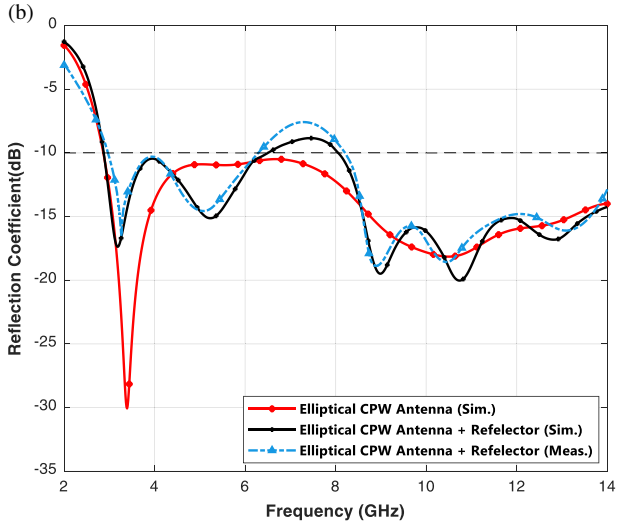

FIGURE 7. (a) Fabricated antenna. (b) Return loss simulated vs measured with reflector plate.

3.4. Effect of All Elliptical Elements' Radius ($R_X = -2$ to 2)

Impact has been observed on radius(s) $R_{x2} = 5$ to 9 mm, $R_{x3} = 3$ to 7 mm, and $R_{x4} = 2$ to 4 mm of different elliptical radiating patch elements in the X-axis by varying this parameter. As (R_X) increases the width of patch element increases, so a significant variation in reflection coefficient has been found at a moderate value of $Rx = 1$ mm makes $R_{x1} = 10$ mm, $R_{x2} = 8$ mm, $R_{x3} = 6$ mm and $R_{x4} = 4$ mm achieving accurate impedance matching between the radiating patch and the ground which holds significant importance. The impact of the patch element radius R_X on antenna performance is illustrated in Figure 6.

3.5. Exploring the Influence of the Space between the Antenna and Reflector on Amplification

The highest achievable gain for the proposed antenna was attained through the adjustment of the gap between the antenna and reflector plane. This parameter is responsible for analyzing the gain. Gap has been varied from 8 mm to 12 mm, and it is found that the moderate value 10 m is good for getting the peak gain of 8.759 dBi at 6 GHz from the normal gain of 2.8 dBi.

3.6. Effect of Gap between Antenna and Reflector (Gap) on Directivity

Through fine-tuning the distance separating the antenna from the reflector plane, we have achieved the utmost level of directivity achievable for the envisioned antenna design. This parameter is responsible for analyzing the gain. Gap has been varied from 8 mm to 12 mm, and it is found that the moderate value is 10 mm, suitable for getting the maximum directivity of 9.537 dBi at 6 GHz from normal directivity of 3.44 dBi at 6 GHz.

4. RESULT ANALYSES AND DISCUSSION

In this section, we evaluate the performance of the proposed antenna through an analysis of the reflection coefficient, S_{11}.

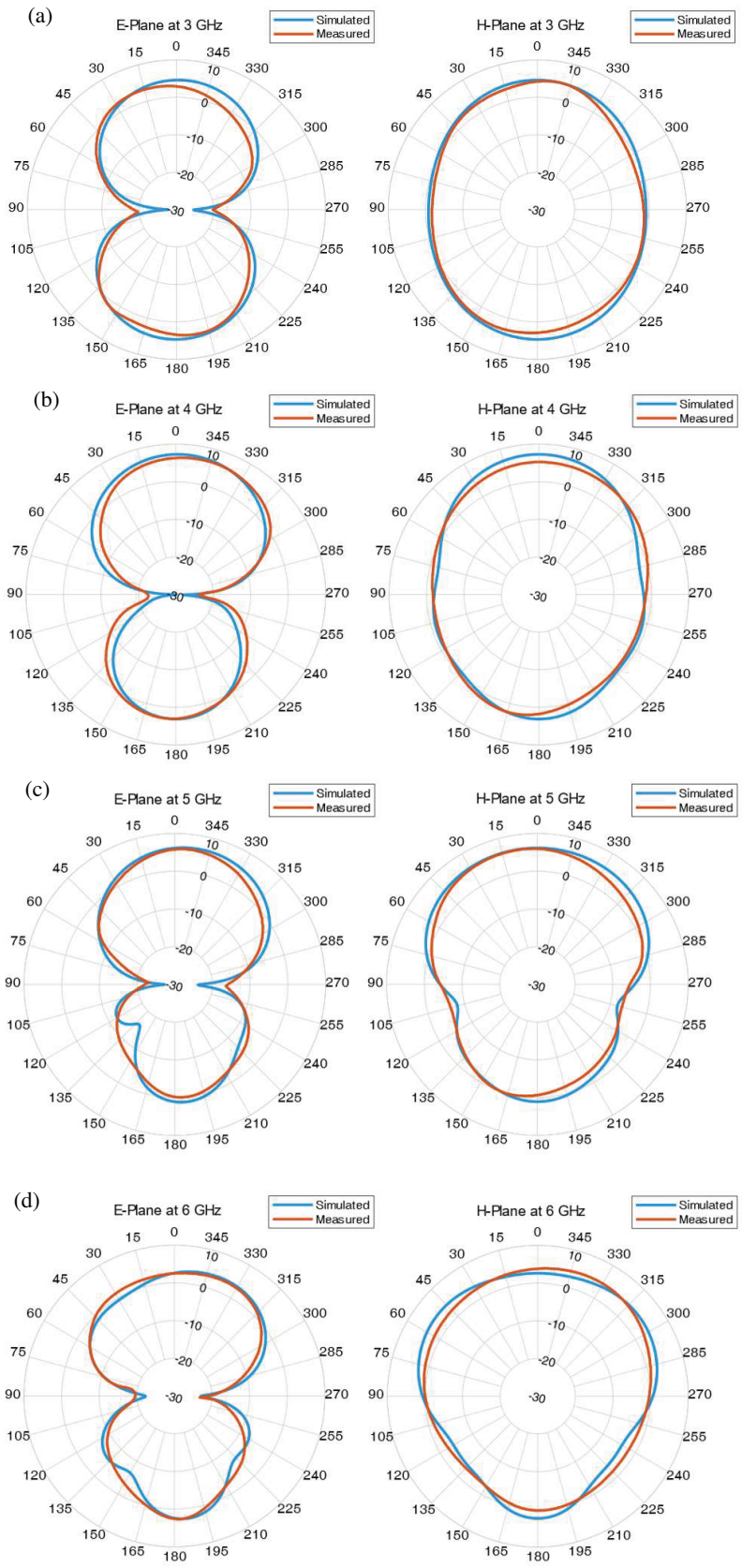

FIGURE 8. Radiation patterns for the E-field and H-field in 2D will be analyzed across frequencies of (a) 3, (b) 4, (c) 5, and (d) 6 GHz.

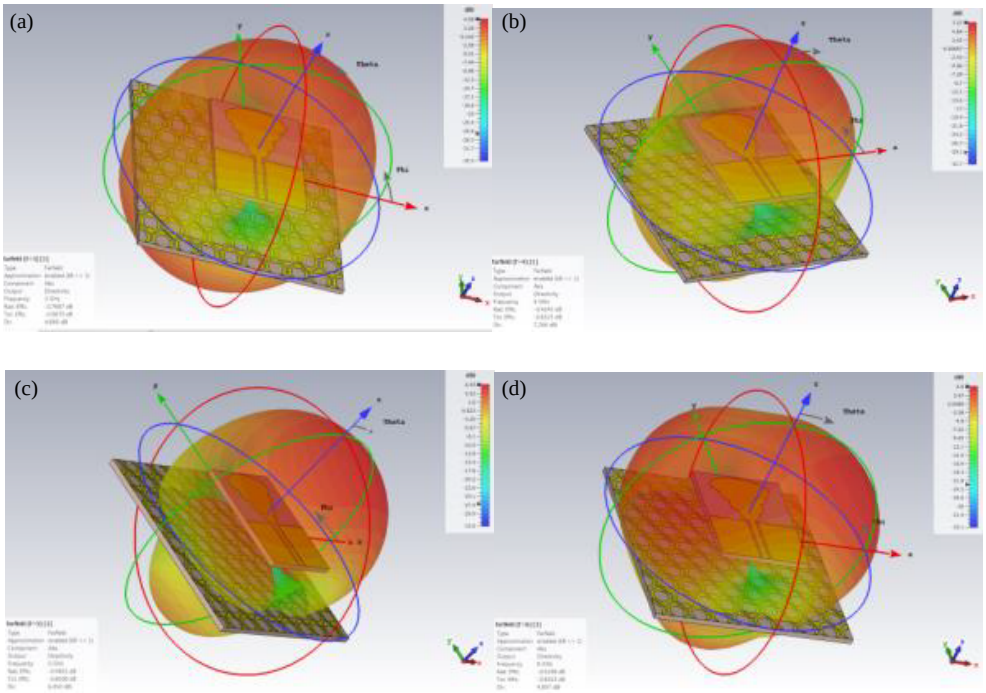

FIGURE 9. 3D view of radiation pattern with antenna structure at (a) 3, (b) 4, (c) 5 and (d) 6 GHz frequency.

In the first band, the lower cutoff frequency (simulated) is denoted as $f_{l1} = 2.87$ GHz, while the higher cutoff frequency is $f_{h1} = 6.48$ GHz. In the second band, the simulated cutoff frequency is $f_{l2} = 8.064$ GHz, and the higher cutoff frequency is $f_{h2} = 14$ GHz. The first resonance frequencies are measured at $f_{r1} = 3.188$ GHz, $f_{r2} = 5.228$ GHz, $f_{r3} = 8.948$ GHz, and $f_{r4} = 10.736$ GHz, exhibiting maximum return losses of -19.486 dB and -20.026 dB, respectively, as depicted in Figure 2(b). The proposed antenna's overall dimensions are $59\times59\times11.67$ mm^2. It offers a fractional bandwidth of 77.22% from 2.87 to 6.48 GHz and 53.80% from 8.064 to 14 GHz.

A striking achievement of an 8.759 dBi peak gain and an outstanding maximum directivity of 9.537 dBi were reached specifically at the frequency of 6 GHz. Figure 7(a) illustrates the fabricated prototype of the antenna featuring a reflector plate. Additionally, Figure 7(b) displays a comparison of the return loss characteristics between the elliptical CPW antenna on its own and when it is combined with the reflector, showcasing the measured results.

4.1. Fractional Bandwidth

The fractional simulation bandwidth of 77.22% from 2.87 to 6.48 GHz and 53.80% from 8.064 to 14 GHz frequency band were obtained from simulated results.

$$\begin{aligned}\text{First Band FB} &= 2\times\left(\frac{f_H - F_L}{f_H + F_L}\right)\%\\ &= 200\times\left(\frac{6.48-2.87}{6.48+2.87}\right)\%\\ &= 200\times\left(\frac{3.61}{9.35}\right)\%\end{aligned}$$

$$\text{Antenna Bandwidth} = 77.22\%$$

$$\begin{aligned}\text{Second Band FB} &= 2\times\left(\frac{f_H - F_L}{f_H + F_L}\right)\%\\ &= 200\times\left(\frac{14-8.064}{14+8.064}\right)\%\\ &= 200\times\left(\frac{5.936}{22.064}\right)\%\end{aligned}$$

$$\text{Antenna Bandwidth} = 53.80\%$$

4.2. Radiation Pattern Analysis of MMES Antenna's E-Field and H-Field in Two Dimensions

The MMES microstrip antenna's two-dimensional E-field and H-field radiation pattern has been analyzed at 3, 4, 5, and 6 GHz depicted in Figure 8. At frequency 3 and 4 GHz bidirectional radiation pattern and at 5 and 6 GHz frequency, the distorted bidirectional radiation patterns have been found in E-field. In H-field at 4, 5, and 6 GHz, the quasi-omni directional radiation pattern has been achieved.

4.3. Radiation Patterns of MMES Antenna's E-Field and H-Field in Three Dimensions

Analyzed in Figure 9, the three-dimensional E-field and H-field radiation patterns of the MMES microstrip antenna were thoroughly examined across frequencies of 3, 4, 5, and 6 GHz.

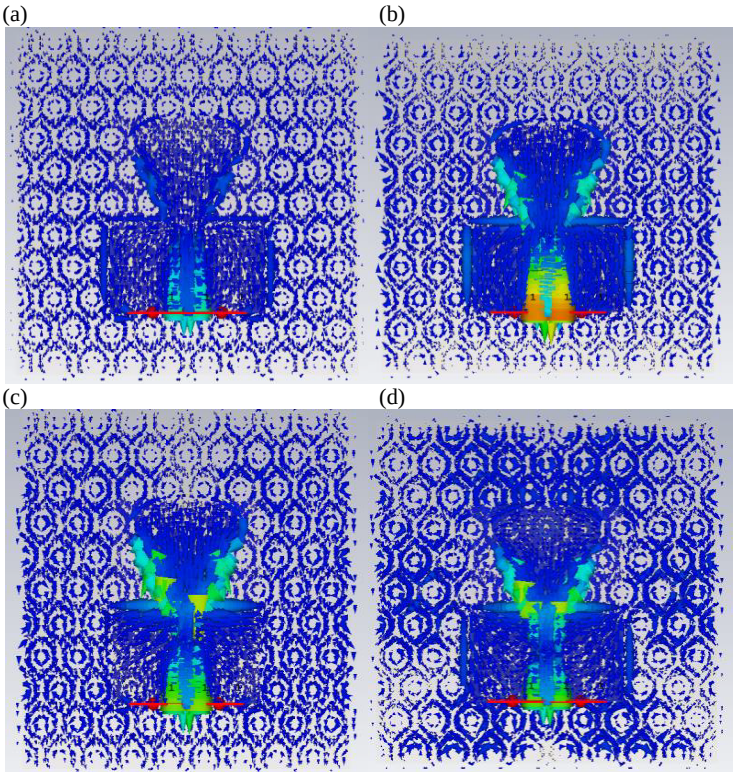

FIGURE 10. Depicts the surface current distribution of the antenna across various frequencies: (a) 3 GHz, (b) 4 GHz, (c) 5 GHz, and (d) 6 GHz.

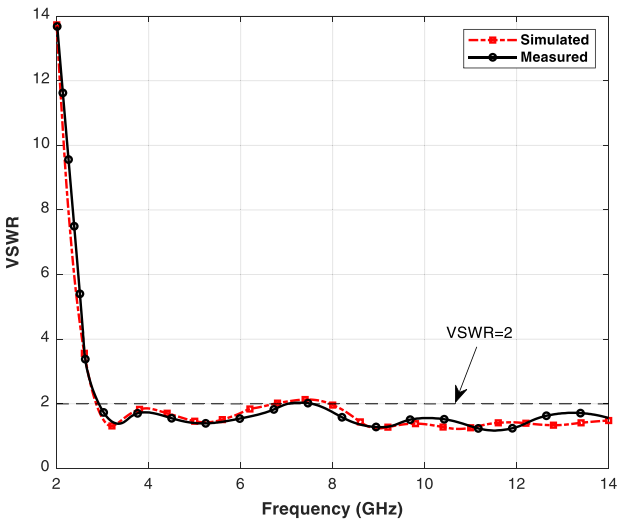

FIGURE 11. VSWR of antenna.

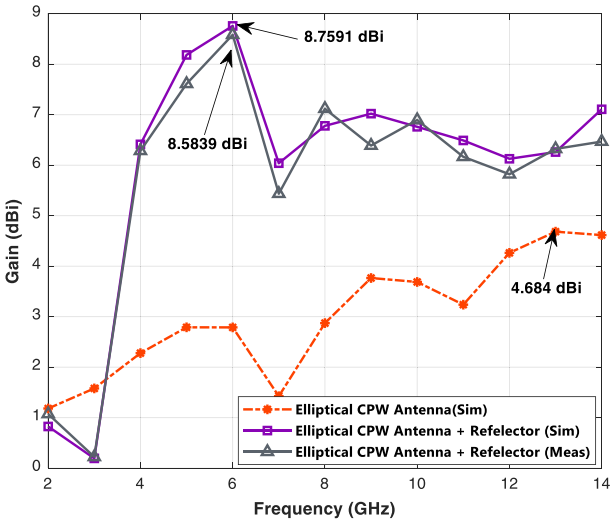

FIGURE 12. Gain of antenna.

At frequency 3 and 4 GHz bidirectional radiation pattern and at 5 and 6 GHz frequency distorted bidirectional radiation pattern have been found in E-field. In H-field at 4, 5, and 6 GHz, the quasi-omnidirectional radiation pattern has been achieved.

4.4. Distribution of Surface Current in MMES Antenna

An analysis of the antenna's spatial layout is showcased in Figure 10 across different frequencies 3 GHz (a), 4 GHz (b), 5 GHz (c), and 6 GHz (d). The current vectors demonstrate a notable focal point at the bottom of the microstrip feed line, while showcasing dispersion at other frequency ranges. For an in-depth understanding, Table 2 offers a comparative study between the gain and directivity of the newly proposed antenna and earlier designs.

4.5. Voltage Standing Wave Ratio (VSWR)

The examination of the VSWR concerning the MMES microstrip antenna illustrates a consistent trend of values below

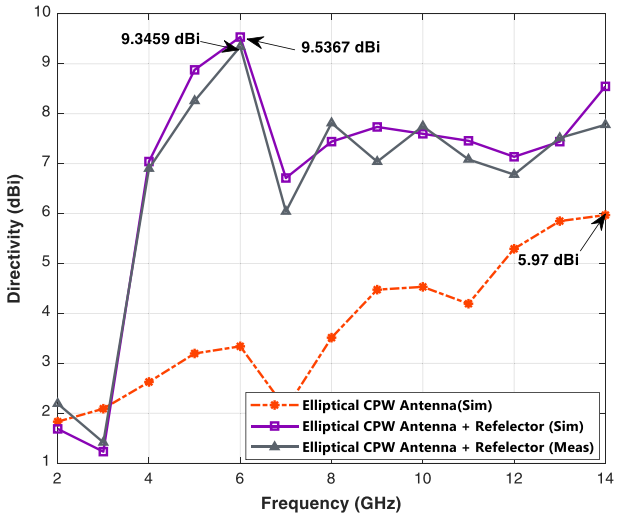

FIGURE 13. Directivity of antenna.

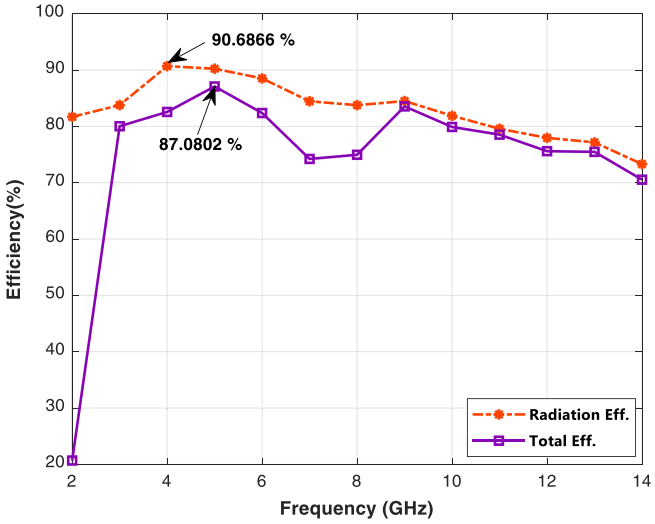

FIGURE 14. Radiation and total antenna efficiency.

TABLE 2. Assessing the antenna gain proposed against high-gain antennas.

Ref	Technique/ Structure	Dimension Size (mm)	F_{low} to F_{High}	Peak Realized Gain
[11]	DGS, Monopole	28.03×23.45×5.35 mm^3	4.775 to 5.049 GHz	5.49dB (G) 7.12dB (D)
[12]	CPW, AMC	34×30mm	2 to 2.6 GHz	6.68 dBi
[13]	Meta surface	105×105×8.4mm^3	2.29 to 2.6 GHz	8.68 dBi
[10]	AMC	47mm ×36 mm	2.37-2.47, 3.51-3.67, 5.7-6.01 GHz	8.6 dB
[14]	CPW, FSS	44×44×33.5mm^3	3.05 to 13.4 GHz	5.5-8.5dBi
[15]	CPW, FSS	110×140×70 mm^3	3.8 to 10.6 GHz	8dBi
Proposed Work	CPW, FSS	59×59×11.635 mm^3	2.87 to 6.48 GHz 8.064 to 14 GHz.	8.759 dBi (G) 9.537 dBi (D)

two within the frequency spans of 2.87 to 6.48 GHz and 8.064 to 14 GHz. This affirms the exemplary performance of the antenna proposed, as illustrated in Figure 11.

4.6. Gain and Directivity of Antenna

The compact mixed multi-elliptical shape microstrip patch antenna has achieved the top gain of 8.759 dBi and directivity of 9.537 dBi with compact size as shown in Figure 12 and Figure 13 and is found as a good candidate for 2.87 to 6.48 GHz and 8.064 to 14 GHz wireless applications such as WiMAX and WLAN applications.

4.7. Antenna Efficiency

Figure 14 showcases the plot illustrating the effectiveness of the antenna. Within the frequency span of 4 to 6 GHz, the suggested antenna showcases an impressive radiation efficiency of 90.68%. Additionally, the highest total efficiency of 87.08% is observed precisely at the 5 GHz frequency.

5. CONCLUSION AND FUTURE SCOPE

The presented study delves into an innovative design featuring a mixed multi-elliptical shape radiating patch antenna, enhanced by a hexagon cell-loaded array reflector with octagon slots. This work utilizes the CPW design, implemented on an FR-4 substrate. Dual-bands from 2.88 to 6.5 GHz frequency of 76.95% and 53.85% from 8.06 to 14 GHz fractional bandwidth have been achieved. At 5.1 GHz, the maximum reflection coefficient ($S_{11}|$) -20 dB was discovered, and at 10.74 GHz, five resonance frequencies (3.188 GHz, 5.228 GHz, 8.984 GHz, 10.736 GHz, and 12.824 GHz) were established. The inclusion of an octagon slot array reflector beneath the antenna within the hexagon cell aims to enhance both the gain and directivity of the intended antenna system. At a frequency of 6 GHz, the augmented reflector demonstrates a peak gain of 8.759 dBi, significantly surpassing the initial gain of 2.8 dBi without the reflector. Furthermore, the maximum directivity reaches 9.537 dBi at 6 GHz, a substantial improvement from the initial 3.44 dBi. The antenna's overall dimensions measure $59 \times 59 \times 11.67\,mm^2$. Through both simulated and measured

results, it becomes evident that this antenna design stands as an optimal choice for applications such as BT, WLAN, and WiMAX. Potential enhancements in the future may involve modifications in the reflector plate's dimensions and alterations in the cell geometry to further elevate the antenna's gain. Employing a substrate material with an ideal dielectric constant remains pivotal for continued gain augmentation.

REFERENCES

[1] Juyal, P. and L. Shafai, "A high-gain single-feed dual-mode microstrip disc radiator," *IEEE Transactions on Antennas and Propagation*, Vol. 64, No. 6, 2115–2126, Jun. 2016.

[2] Feresidis, A. P. and J. C. Vardaxoglou, "High gain planar antenna using optimised partially reflective surfaces," *IEE Proceedings — Microwaves, Antennas and Propagation*, Vol. 148, No. 6, 345–350, Dec. 2001.

[3] Foroozesh, A. and L. Shafai, "Investigation into the effects of the patch-type FSS superstrate on the high-gain cavity resonance antenna design," *IEEE Transactions on Antennas and Propagation*, Vol. 58, No. 2, 258–270, 2010.

[4] Foroozesh, A. and L. Shafai, "On the characteristics of the highly directive resonant cavity antenna having metal strip grating superstrate," *IEEE Transactions on Antennas and Propagation*, Vol. 60, No. 1, 78–91, Jan. 2012.

[5] Feresidis, A. P., G. Goussetis, S. H. Wang, and J. C. Vardaxoglou, "Artificial magnetic conductor surfaces and their application to low-profile high-gain planar antennas," *IEEE Transactions on Antennas and Propagation*, Vol. 53, No. 1, 209–215, Jan. 2005.

[6] Mateo-Segura, C., G. Goussetis, and A. P. Feresidis, "Sub-wavelength profile 2-D leaky-wave antennas with two periodic layers," *IEEE Transactions on Antennas and Propagation*, Vol. 59, No. 2, 416–424, Feb. 2011.

[7] Zhou, L., H. Q. Li, Y. Q. Qin, Z. Y. Wei, and C. T. Chan, "Directive emissions from subwavelength metamaterial-based cavities," *Applied Physics Letters*, Vol. 86, No. 10, 101 101–1–3, Mar. 2005.

[8] Ourir, A., A. D. Lustrac, and J.-M. Lourtioz, "All-metamaterial-based subwavelength cavities (λ/60) for ultrathin directive antennas," *Applied Physics Letters*, Vol. 88, No. 8, 084103, Feb. 2006.

[9] Al-Gburi, A. J. A., I. B. M. Ibrahim, M. Y. Zeain, and Z. Zakaria, "Compact size and high gain of CPW-fed UWB strawberry artistic shaped printed monopole antennas using FSS single layer reflector," *IEEE Access*, Vol. 8, 92 697–92 707, 2020.

[10] Gan, W., X. Lu, J. Yang, Z. Zhang, F. Liu, and S. Yang, "Design of the triple band microstrip antenna with AMC reflector," in *2020 Asia Conference on Computers and Communications (ACCC)*, 2020.

[11] Olawoye, T. O. and P. Kumar, "A high gain microstrip patch antenna with slotted ground plane for sub-6 GHz 5G communications," in *2020 International Conference on Artificial Intelligence, Big Data, Computing and Data Communication Systems (icABCD)*, 1–6, 2020.

[12] Yuan, Y.-N., J.-J. Feng, and X.-L. Xi, "Design of wearable antenna with compact artificial magnetic conductor reflecting plate," in *2017 Sixth Asia-Pacific Conference on Antennas and Propagation (APCAP)*, 1–3, Oct. 2017.

[13] Chung, K. L. and S. Chaimool, "Broadside gain and bandwidth enhancement of microstrip patch antenna using a MNZ-metasurface," *Microwave and Optical Technology Letters*, Vol. 54, No. 2, 529–532, 2012.

[14] Kundu, S., A. Chatterjee, S. K. Jana, and S. K. Parui, "A compact umbrella-shaped UWB antenna with gain augmentation using frequency selective surface," *Radioengineering*, Vol. 27, No. 2, 448–454, Jun. 2018.

[15] Abdulhasan, R. A., R. Alias, K. N. Ramli, F. C. Seman, and R. A. Abd-Alhameed, "High gain CPW-fed UWB planar monopole antenna-based compact uniplanar frequency selective surface for microwave imaging," *International Journal of RF and Microwave Computer-Aided Engineering*, Vol. 29, No. 8, e21757, Aug. 2019.

[16] Yuan, Y., X. Xi, and Y. Zhao, "Compact UWB FSS reflector for antenna gain enhancement," *IET Microwaves, Antennas & Propagation*, Vol. 13, No. 10, 1749–1755, Aug. 2019.

[17] Tahir, F. A., T. Arshad, S. Ullah, and J. A. Flint, "A novel FSS for gain enhancement of printed antennas in UWB frequency spectrum," *Microwave and Optical Technology Letters*, Vol. 59, No. 10, 2698–2704, Oct. 2017.